

Soft colloids make strong glasses

Johan Mattsson^{1†}, Hans M. Wyss^{1†}, Alberto Fernandez-Nieves^{1†}, Kunimasa Miyazaki^{2†}, Zhibing Hu³, David R. Reichman² & David A. Weitz¹

Glass formation in colloidal suspensions has many of the hallmarks of glass formation in molecular materials^{1–5}. For hard-sphere colloids, which interact only as a result of excluded volume, phase behaviour is controlled by volume fraction, ϕ ; an increase in ϕ drives the system towards its glassy state, analogously to a decrease in temperature, T , in molecular systems. When ϕ increases above $\phi^* \approx 0.53$, the viscosity starts to increase significantly, and the system eventually moves out of equilibrium at the glass transition, $\phi_g \approx 0.58$, where particle crowding greatly restricts structural relaxation^{1–4}. The large particle size makes it possible to study both structure and dynamics with light scattering¹ and imaging^{3,4}; colloidal suspensions have therefore provided considerable insight into the glass transition. However, hard-sphere colloidal suspensions do not exhibit the same diversity of behaviour as molecular glasses. This is highlighted by the wide variation in behaviour observed for the viscosity or structural relaxation time, τ_α , when the glassy state is approached in supercooled molecular liquids⁵. This variation is characterized by the unifying concept of fragility⁵, which has spurred the search for a ‘universal’ description of dynamic arrest in glass-forming liquids. For ‘fragile’ liquids, τ_α is highly sensitive to changes in T , whereas non-fragile, or ‘strong’, liquids show a much lower T sensitivity. In contrast, hard-sphere colloidal suspensions are restricted to fragile behaviour, as determined by their ϕ dependence^{1,6}, ultimately limiting their utility in the study of the glass transition. Here we show that deformable colloidal particles, when studied through their concentration dependence at fixed temperature, do exhibit the same variation in fragility as that observed in the T dependence of molecular liquids at fixed volume. Their fragility is dictated by elastic properties on the scale of individual colloidal particles. Furthermore, we find an equivalent effect in molecular systems, where elasticity directly reflects fragility. Colloidal suspensions may thus provide new insight into glass formation in molecular systems.

The concept of fragility is best summarized in a renormalized Arrhenius plot, where the temperature is rescaled by the glass-transition temperature, T_g , and fragility is defined by the logarithmic slope at T_g (ref. 5). This representation highlights the wide variation in behaviour of molecular liquids, ranging from strong to fragile, and provides a unifying conceptual framework. An understanding of the physical origin of fragility, however, is lacking. The fragility of colloidal suspensions must be defined by their concentration dependence rather than by their T dependence. With this definition, colloidal hard-sphere suspensions are restricted to fragile behaviour and the absence of a wider range of fragilities limits their versatility as a model system of the glass transition.

We studied aqueous suspensions of deformable microgel particles of varying elasticity (Methods Summary). To obtain a measure of

their elasticity, we probed the compressibility of individual particles by determining the change in particle size with both osmotic pressure and temperature (Supplementary Information). We determined the particle concentrations, ζ , from the known polymer concentrations of the microgel suspensions. For hard-sphere suspensions, the particle concentration is quantified by the volume fraction, $\phi = nV_p$, where n is the number density of particles and V_p is their volume. However, because the microgel particles are deformable, their volume is not fixed and ϕ is no longer a good measure of concentration. Instead, we used $\zeta = nV_0$, where $V_0 = 4\pi R_0^3/3$ is the volume of an undeformed particle of radius R_0 measured in dilute suspension; ζ is always proportional to the polymer concentration. At low concentrations, where V_p is independent of concentration, $\zeta = \phi$ and soft microgels can be treated as hard spheres⁷. To calibrate the measurement of ζ , we determined the viscosity at low concentrations and used the Einstein expression to directly link the polymer concentration and ζ (Supplementary Information). As ζ increases above $\phi_{\text{RCP}} \approx 0.63$, corresponding to the random close packing of undeformed spheres, the particles must shrink; we confirmed this behaviour using static light scattering, which shows a systematic shift of the first peak in the effective structure factor (Supplementary Information).

We studied the dynamics of the microgel suspensions for fixed T and varying ζ using dynamic light scattering (Supplementary Information). The behaviour observed for deformable microgel particles is qualitatively similar to that of hard spheres: for the lowest ζ value, we find a monomodal decay of the intermediate scattering function, $g_1(t)$, which captures diffusion of particles in a dilute suspension, as shown for microgels with ‘intermediate’ stiffness and $R_0 = 92$ nm in Fig. 1a. As ζ increases, there are marked changes in the dynamics and we observe a two-step relaxation, characteristic of glass-forming materials upon approach to the glass transition⁵; the fast initial decay is only weakly dependent on ζ , whereas the final decay, which reflects structural relaxation, depends strongly on ζ . The final decay is well described by a stretched exponential, $g_1(t) \propto \exp(-t/\tau)^\beta$, where τ is the relaxation time and β is the stretching exponent. Moreover, as for hard spheres, the final decay can be superimposed for different values of ζ onto a single master curve by rescaling the decay times, as shown in Fig. 1b. We find that $\beta = 0.6$, as demonstrated in Fig. 1e. A corresponding superposition of the shape of the structural relaxation is often possible for molecular liquids near their glass-transition temperature, where it is referred to as time–temperature superposition⁵.

Unlike hard-sphere suspensions, the microgels are not dynamically arrested at $\zeta \approx 0.63$. Instead, it is necessary to consider much higher ζ values, whereupon the final decay eventually exceeds any experimentally accessible timescale, ultimately resulting in formation of a glass, as shown in Fig. 1a. To quantify the ζ dependence of the final decay, we determined the average structural relaxation time, $\tau_\alpha = (\tau/\beta)\Gamma(1/\beta)$,

¹Department of Physics and Harvard School of Engineering and Applied Sciences, Harvard University, Cambridge, Massachusetts 02138, USA. ²Department of Chemistry, Columbia University, New York, New York 10027, USA. ³Department of Physics, University of North Texas, Denton, Texas 76203, USA. †Present addresses: Department of Applied Physics, Chalmers University of Technology, SE-412 96 Göteborg, Sweden (J.M.); TU Eindhoven, Institute for Complex Molecular Systems and Department of Mechanical Engineering, PO Box 513, 5600 MB Eindhoven, The Netherlands (H.M.W.); School of Physics, Georgia Institute of Technology, Atlanta, Georgia 30332, USA (A.F.-N.); Institute of Physics, University of Tsukuba, Tsukuba 305-8571, Japan (K.M.).

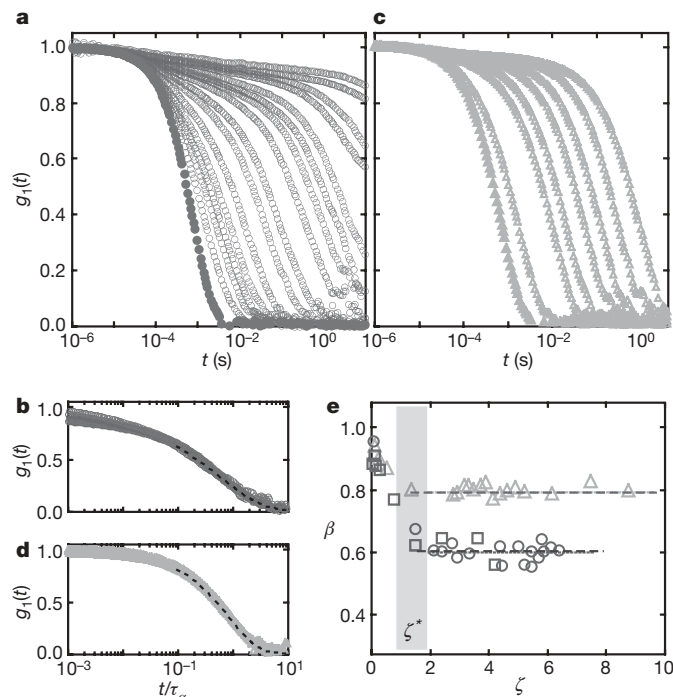


Figure 1 | Dynamics of microgel suspensions. **a, c,** Plots of $g_1(t)$ for intermediate (**a**) and soft (**c**) microgels at $Q = 23\mu\text{m}^{-1}$, where ζ ranges from 8×10^{-4} to 8.1 and from 0.15 to 9.4, respectively. Filled symbols indicate data for $\zeta < \zeta^*$. **b, d,** Time–concentration superposition for intermediate (**b**) and soft (**d**) microgels. The dashed lines are stretched exponential fits. **e,** The stretching exponent β remains constant for values of ζ greater than ζ^* (the range of ζ^* is indicated by the shaded region) for both intermediate (circles, $R_0 = 92$ nm; squares, $R_0 = 168$ nm) and soft (triangles, $R_0 = 80$ nm) microgels.

where Γ denotes the gamma function. We used a fixed value of the scattering vector, Q , for each sample even though the particle size, R , and hence QR , vary slightly with ζ . In sharp contrast to the behaviour of hard spheres, where small changes in volume fraction lead to pronounced slowing of the structural relaxation, the dynamic arrest for microgel suspensions stretches over a wide range of ζ values. This difference is highlighted by a comparison of the ζ dependence of τ_z for a ‘stiff’ hard-sphere-like microgel⁸ (Fig. 2a, diamonds) with that

for our intermediate soft microgels (Fig. 2a, circles and squares). We have rescaled the relaxation times by a constant, k (Supplementary Information), to compensate for the different diffusion timescales in the dilute limit and for the differences in QR_0 .

For each microgel sample, we also determined the frequency-dependent shear moduli, $G'(\omega)$ and $G''(\omega)$, by oscillatory rheology; G' has a plateau at high frequencies and a low-frequency structural relaxation (Supplementary Information), strongly reminiscent of the behaviour of concentrated hard-sphere suspensions². We determined τ_z as the timescale corresponding to the frequency for which $G' = G''$ and observed the same ζ dependence of τ_z as was observed from light scattering, as shown by the plus symbols in Fig. 2a. Moreover, the viscosity of the microgel suspensions, determined at sufficiently low shear rates to preclude shear thinning, can also be directly scaled onto the relaxation-time data. Thus, the ζ dependence characterizing structural relaxation is robust, as it is independently determined by several different methods. To describe the relaxation-time data, both for the intermediate and the stiff microgels, we used a Vogel–Fulcher–Tammann (VFT) function⁵, $\tau_z = \tau_0 \exp(A\zeta/(\zeta_0 - \zeta))$, where ζ_0 sets the apparent divergence, A controls the growth of τ_z on approach to ζ_0 and τ_0 is the characteristic relaxation time for low values of ζ . This empirical function, with $1/\zeta$ exchanged for T , provides a good description of the T dependence of τ_z for supercooled molecular liquids near their glass transition⁵. These data thus further confirm that for suspensions of soft particles, ζ plays a role analogous to that of $1/T$ in molecular systems.

Our experiments show that for soft colloidal particles, the approach to the glass transition upon varying ζ is more gradual than for hard spheres; this is reminiscent of the behaviour found in molecular liquids upon varying T , where different fragilities are observed. We therefore propose that the concept of fragility can be extended to colloidal systems through control of particle elasticity, provided that we use ζ in the colloidal systems. To test this hypothesis, we investigated the behaviour of even softer microgels (Supplementary Information). These had similar behaviour in their dynamics, including a nearly exponential decay of $g_1(t)$ at low ζ values and a two-step decay with stretched-exponential behaviour of the final decay for ζ values greater than a certain crossover concentration, ζ^* (Supplementary Information), as shown in Fig. 1c. Moreover, the final decay can again be scaled onto a single master curve, as shown in Fig. 1d; however, $\beta = 0.8$, which is higher than for our microgel of intermediate stiffness (Fig. 1e). When τ_z is plotted as a function of ζ , we find exponential behaviour, $\tau_z = \tau_0 \exp(C\zeta)$, where

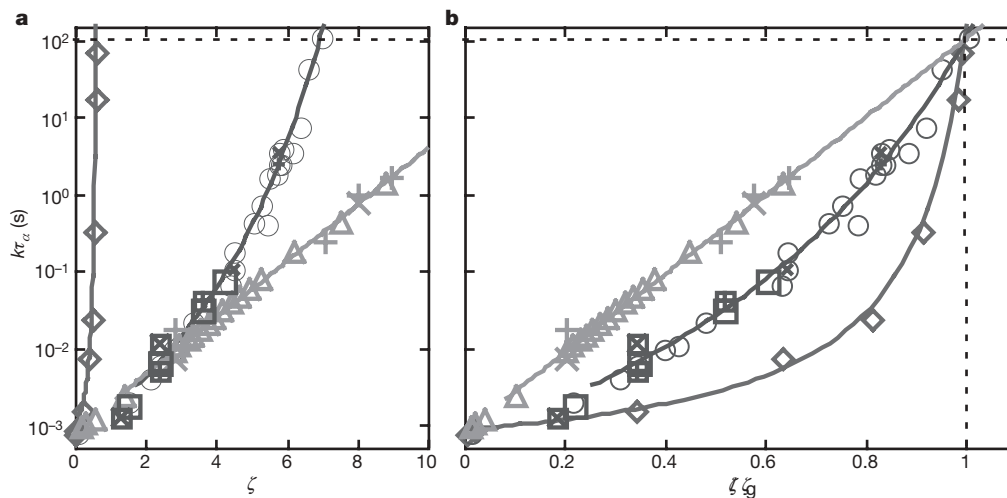


Figure 2 | Fragility range for colloids. **a,** Plot of $k\tau_z$ versus ζ for stiff (diamonds, $R_0 = 95$ nm)⁸, intermediate (empty circles, $R_0 = 92$ nm) and soft (triangles, $R_0 = 80$ nm) microgels, where k is chosen to collapse the data onto those of the intermediate sample at low ζ values. Data for a second intermediate sample (empty squares, $R_0 = 168$ nm) scale onto those of the

first for $\zeta > \zeta^*$, as expected. Rescaled shear viscosities (intermediate: crosses in circles, $R_0 = 92$ nm, and crosses in squares, $R_0 = 168$ nm; soft: crosses, $R_0 = 80$ nm) and rheological structural relaxation times (intermediate: pluses in circles, $R_0 = 92$ nm, and pluses in squares, $R_0 = 168$ nm; soft: pluses, $R_0 = 80$ nm). **b,** Same as **a**, with ζ normalized by $\zeta_g = \zeta(\tau_z = 100$ s).

C is a constant, as shown by the triangles in Fig. 2a; the same behaviour is observed in measurements of both rheology (pluses) and viscosity (crosses). This exponential dependence is analogous to the Arrhenius behaviour typically observed in strong molecular glass-formers such as silica, but here with T exchanged for $1/\zeta$; the exponential dependence also corresponds to VFT behaviour with $\zeta_0 \gg \zeta$.

We thus confirm our hypothesis that the concept of fragility can be extended to colloidal systems by control of the particle elasticity and through the variation of ζ . Interestingly, we also find the smallest stretching exponent for the sample with the strongest dynamic behaviour. This observation is reminiscent of that seen in molecular systems, where a correlation between higher β values and stronger dynamic behaviour has been reported⁵.

To explore the analogy between soft colloidal suspensions and molecular glass-formers further, we represent our data in a rescaled Arrhenius plot in a fashion similar to that used for molecular glasses⁵. For molecular glass-formers, the abscissa of this plot is typically scaled by T_g , defined as the temperature ($\tau_\alpha = 100$ s) (ref. 5), where the structural relaxation is no longer experimentally accessible. By analogy, we rescale the concentration ζ by $\zeta_g = \zeta(\tau_\alpha = 100$ s) to obtain the corresponding plot for colloids. We view the slope of the data at ζ_g as the fragility. As in molecular liquids, the fragility varies continuously from strong to fragile, as shown in Fig. 2b; for the microgels, it is controlled by particle elasticity. We note that the ratio ζ_g/ζ^* is smaller the more fragile is the behaviour, just as the ratio T^*/T_g is smaller the more fragile is a molecular liquid⁵; here, T^* denotes the crossover temperature (Supplementary Information). Changes in molecular motions, characteristic of a deeply supercooled liquid, are first observed at T^* , corresponding to ζ^* in colloids. We note that pressure-dependent measurements on molecular liquids can be summarized by a similar type of plot of viscosity as a function of inverse volume rescaled by the glass-transition volume; this suggests a connection between volume-dependent fragility in colloids and molecular liquids⁹.

To investigate the role of particle elasticity in the dynamic arrest, we used oscillatory rheology to determine the concentration dependence of the elastic modulus on a timescale characterizing local particle motion, $G_p(\zeta)$ (Methods Summary). We determined the elastic energy on a particle length scale $G_p(\zeta)V_p$, where V_p is the volume of the deformable particles, is estimated for $\zeta \geq \zeta^*$ to be $V_p = (\zeta/\zeta^*)4\pi R_0^3/3$. This elastic energy dominates over thermal energy near the glass transition for all samples, as demonstrated by the dependence of $G_p(\zeta)V_p/k_B T$ on ζ/ζ^* (Fig. 3a; k_B , Boltzmann constant); here we scaled by ζ^* to mark the onset of the relevant dynamic range. Moreover, we observe a direct correlation between the growth of this energy ratio and fragility: the softer the particles, the stronger their suspension behaviour and, correspondingly, the weaker the growth of elastic energy with ζ as it increases above ζ^* . This suggests that the

suspension elasticity on the particle scale controls the dynamics above ζ^* and, thus, determines the fragility. To compare data for different fragilities, we determined the volumes $V^* = \gamma V_p$ (Supplementary Information), where γ is a constant chosen to make the elastic energy equal the thermal energy at ζ^* . The energy ratios increase more quickly as the fragility increases, as shown by a plot of $G_p(\zeta)V^*/k_B T$ as a function of ζ/ζ^* (Fig. 3b). We find that V^* is smaller than the particle volume for all samples, confirming that the elasticity on local length scales determines the fragility.

For supercooled liquids, there are apparent correlations between fragility and the behaviour of the elastic properties^{10–15} as expressed, for example, by the non-ergodicity parameter¹², the bulk and shear moduli^{10,11,13–15} or the strength of the boson peak¹⁴; however, the underlying origin of fragility in supercooled liquids remains unresolved. On the basis of our results for deformable colloids, we explored the possibility that the elastic energy correlates with fragility also for molecular systems. We determined the elastic energy, $G_\infty(T)V_{\text{liq}}^*$, where $G_\infty(T)$ denotes the high-frequency shear modulus as measured by Brillouin light scattering and V_{liq}^* , the volume for each liquid, is chosen such that $G_\infty(T^*)V_{\text{liq}}^* = k_B T^*$. We find that $G_\infty(T)V_{\text{liq}}^*/k_B T$ as a function of T^*/T is well described by a linear function for each liquid; moreover, an increase in fragility is accompanied by a more pronounced slope, as shown in Fig. 3c. In addition, V_{liq}^* is smaller than the molecular size for all liquids (Supplementary Information), in further analogy with our findings for soft, deformable colloids. The striking qualitative similarity in the behaviour of the elastic energies of molecular systems and colloidal suspensions confirms the important role of elasticity in determining fragility. Our results thus suggest that thermal activation controls fragility, with a ζ -dependent elastic energy for colloids, corresponding to a T -dependent elastic energy for molecular liquids.

Structural relaxation in molecular glass-formers can be described by thermal activation within a complex energy landscape, which reflects the possible configurations of the system; fragility is reflected in the detailed topology of this energy landscape^{5,16}. Fragility might also have a parallel in the temperature dependence of purely thermodynamic properties, such as entropy^{17,18}. Interestingly, theoretical work for colloidal hard-sphere systems suggests that the ϕ variation of the local configurational properties is surprisingly similar to the T variation of the corresponding configurational properties of molecular liquids¹⁹. This implies that the concept of fragility is far more general than previously believed. Our work provides more evidence for this by demonstrating that the concept of fragility can be directly extended to suspensions of deformable colloidal particles, where particle concentration controls glass formation. Furthermore, our work suggests that the origin of the variation in fragility resides in the elastic properties of the particles themselves; soft particles lead to strong behaviour and hard particles lead to fragile behaviour.

In molecular glass-formers, strong dynamic behaviour generally reflects a significant degree of directional bonding that is typical of network-forming glass-formers such as silica. By analogy, we speculate that the origin of the behaviour of colloidal suspensions is similar: softer particles are more easily deformed, and as the particles shrink their shapes will increasingly deviate from the spherical, which in turn leads to an increased directionality of interparticle interactions^{20,21}, corresponding to strong behaviour. By contrast, hard particles retain their spherical shape and their interactions are more isotropic, corresponding to fragile behaviour.

The results presented here demonstrate the remarkable similarities between the behaviours of colloidal and molecular glass-formers, and suggest that an improved understanding of glass formation may come from exploring the properties of other soft colloidal systems, such as solutions of star polymers²² and block-copolymer micelles²³.

METHODS SUMMARY

Microgel properties. Our microgel particles consisted of interpenetrated and crosslinked polymer networks of poly(*N*-isopropylacrylamide) and polyacrylic acid²⁴. To study the glass-forming properties of the microgel suspensions, we

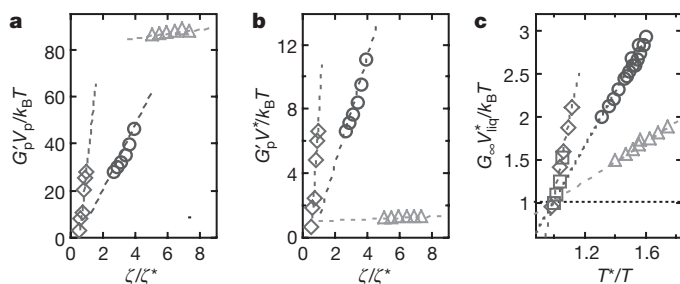


Figure 3 | Elasticity of glass-formers. **a**, Data for soft (triangles) and intermediate (circles) microgel suspensions compared with data for a suspension of model hard spheres (diamonds)²⁵. For the hard-sphere system, $\zeta^* = \phi^* = 0.53$ (ref. 26). The lines are guides to the eye. **b**, A different representation of the data in **a**. **c**, Data for orthoterphenyl (diamonds)²⁷, salol (squares)²⁸, glycerol (circles)²⁹ and silica (triangles)³⁰. The dashed lines are fits to the data. The plot is explained in detail in the text.

used systems with size polydispersities of ~40%, which successfully suppressed crystallization. In addition, our samples were naturally well matched in both density and refractive index, as the particles contained a large fraction of water. The synthesis parameters sensitively affected the elastic properties of the microgel particles themselves. We determined the elastic properties by investigating the change in particle size with osmotic pressure or with temperature (Supplementary Information).

Elasticity of the microgel suspensions. The viscoelastic shear moduli $G'(\omega)$ and $G''(\omega)$, measured for different suspension concentrations, can be superimposed on a master curve by scaling the frequency. Moreover, the master curves for different suspensions can themselves be superimposed onto one common master curve by scaling the magnitudes of the moduli (Supplementary Information). This behaviour enabled us to determine the elastic response at a frequency corresponding to local particle motion, ω_p , determined as the characteristic rheological timescale at ξ^* (Supplementary Information). For the intermediate and the soft samples, we determined $G_p' = G'(\omega_p)$, the elastic modulus at ω_p , and from G_p' we determined the effective elastic energy per particle, $G_p' V_p$. We compared our results with data for a hard-sphere-like system from ref. 25.

Received 30 April; accepted 21 August 2009.

- van Meegen, W. & Pusey, P. N. Dynamic light-scattering study of the glass transition in a colloidal suspension. *Phys. Rev. A* **43**, 5429–5441 (1991).
- Mason, T. G. & Weitz, D. A. Linear viscoelasticity of colloidal hard sphere suspensions near the glass transition. *Phys. Rev. Lett.* **75**, 2770–2773 (1995).
- Kegel, W. K. & van Blaaderen, A. Direct observation of dynamical heterogeneities in colloidal hard-sphere suspensions. *Science* **287**, 290–293 (2000).
- Weeks, E. R., Crocker, J. C., Levitt, A. C., Schofield, A. & Weitz, D. A. Three-dimensional direct imaging of structural relaxation near the colloidal glass transition. *Science* **287**, 627–631 (2000).
- Angell, C. A., Ngai, K. L., McKenna, G. B., McMillan, P. F. & Martin, S. W. Relaxation in glass-forming liquids and amorphous solids. *J. Appl. Phys.* **88**, 3113–3157 (2000).
- Cheng, Z., Zhu, J., Chaikin, P. M., Phan, S.-E. & Russel, W. B. Nature of the divergence in low shear viscosity of colloidal hard-sphere dispersions. *Phys. Rev. E* **65**, 041405 (2002).
- Stieger, M., Pedersen, J. S., Lindner, P. & Richtering, W. Are thermoresponsive microgels a model system for concentrated colloidal suspensions? A rheology and small-angle neutron scattering study. *Langmuir* **20**, 7283–7292 (2004).
- Bartsch, E., Antonietti, M., Schupp, W. & Sillescu, H. The glass transition dynamics of polymer micronetwork colloids. A mode coupling analysis. *J. Chem. Phys.* **97**, 3950–3963 (1992).
- Herbst, C. A., Cook, R. L. & King, H. E. Jr. Density-mediated transport and the glass transition: high pressure viscosity measurements in the diamond anvil cell. *J. Non-Cryst. Solids* **172–174**, 265–271 (1994).
- Tobolsky, A. V., Powell, R. E. & Eyring, H. in *Frontiers in Chemistry* Vol. 1 (eds Burk, R. E. & Grummit, O.) 125–190 (Interscience, 1943).
- Nemilov, S. V. *Thermodynamic and Kinetic Aspects of the Vitreous State* (CRC Press, 1995).
- Scopigno, T., Ruocco, G., Sette, F. & Monaco, G. Is the fragility of a liquid embedded in the properties of its glass? *Science* **302**, 849–852 (2003).
- Novikov, V. N. & Sokolov, A. P. Poisson's ratio and the fragility of glass-forming liquids. *Nature* **431**, 961–963 (2004).
- Novikov, V. N., Ding, Y. & Sokolov, A. P. Correlation of fragility of supercooled liquids with elastic properties of glasses. *Phys. Rev. E* **71**, 061501 (2005).
- Dyre, J. C. The glass transition and elastic models of glass-forming liquids. *Rev. Mod. Phys.* **78**, 953–972 (2006).
- Sastry, S., Debenedetti, P. G. & Stillinger, F. H. Signatures of distinct dynamical regimes in the energy landscape of a glass-forming liquid. *Nature* **393**, 554–557 (1998).
- Ito, K., Moynihan, C. T. & Angell, C. A. Thermodynamic determination of fragility in liquids and a fragile-to-strong liquid transition in water. *Nature* **398**, 492–495 (1999).
- Martinez, L.-M. & Angell, C. A. A thermodynamic connection to the fragility of glass-forming liquids. *Nature* **410**, 663–667 (2001).
- Brumer, Y. & Reichman, D. R. Mean-field theory, mode-coupling theory, and the onset temperature in supercooled liquids. *Phys. Rev. E* **69**, 041202 (2004).
- Wyart, M. On the rigidity of amorphous solids. *Ann. Phys. Fr.* **30**, 1–96 (2005).
- Shintani, H. & Tanaka, H. Frustration on the way to crystallization in glass. *Nature Mater.* **7**, 870–877 (2008).
- Roovers, J. Concentration dependence of the relative viscosity of star polymers. *Macromolecules* **27**, 5359–5364 (1994).
- Buitenhuis, J. & Förster, S. Block copolymer micelles: viscoelasticity and interaction potential of soft spheres. *J. Chem. Phys.* **107**, 262–272 (1997).
- Xia, X. & Hu, Z. Synthesis and light scattering study of microgels with interpenetrating polymer networks. *Langmuir* **20**, 2094–2098 (2004).
- Shikata, T. & Pearson, D. S. Viscoelastic behaviour of concentrated spherical suspensions. *J. Rheol.* **38**, 601–616 (1994).
- Kumar, S., Szamel, G. & Douglas, J. F. Nature of the breakdown in the Stokes-Einstein relationship in a hard sphere fluid. *J. Chem. Phys.* **124**, 214501 (2006).
- Wang, C. H., Zhu, X. R. & Shen, J. C. Angular and temperature dependence of depolarized and polarized Rayleigh-Brillouin spectra of a supercooled liquid: o-terphenyl. *Mol. Phys.* **62**, 749–764 (1987).
- Enright, G. D. & Stoicheff, B. P. Light scattering from shear modes in liquid salol. *J. Chem. Phys.* **64**, 3658–3665 (1976).
- Scarponi, F., Comez, L., Fioretto, D. & Palmieri, L. Brillouin light scattering from transverse and longitudinal acoustic waves in glycerol. *Phys. Rev. B* **70**, 054203 (2004).
- Polian, A., Vo-Thanh, D. & Richet, P. Elastic properties of a-SiO₂ up to 2300 K from Brillouin scattering measurements. *Europhys. Lett.* **57**, 375–381 (2002).

Supplementary Information is linked to the online version of the paper at www.nature.com/nature.

Acknowledgements We are grateful to J. Zhou for technical assistance, to J. Bergenholtz for complimentary use of his light-scattering equipment and to J.-W. Kim for discussions. This work was supported by the US National Science Foundation and Harvard University's Materials Research Science and Engineering Center; by the Hans Werthén Foundation, the Wenner-Gren Foundation, the Knut and Alice Wallenberg Foundation and the Royal Society of Arts and Sciences in Göteborg (J.M.); by the Ministerio de Ciencia e Innovación and the University of Almería (A.F.-N.); and by KAKENHI (K.M.).

Author Contributions J.M. and H.M.W. designed the study, performed the experiments, analysed and interpreted the data and wrote the manuscript; A.F.-N. designed the study, interpreted the data and wrote the manuscript; Z.H. designed the samples and contributed to the writing of the manuscript; K.M., D.R.R. and D.A.W. each contributed to data interpretation and the writing of the manuscript.

Author Information Reprints and permissions information is available at www.nature.com/reprints. Correspondence and requests for materials should be addressed to J.M. (johanm@chalmers.se).